

Antarctic Permafrost Degassing Revealed By Extensive Soil Gas and CO₂ Flux Survey in Taylor Valley

Livio Ruggiero

National Institute of Geophysics and Volcanology

Alessandra Sciarra (✉ alessandra.sciarra@ingv.it)

National Institute of Geophysics and Volcanology

Adriano Mazzini

Center of Earth Evolution and Dynamics, University of Oslo

Fabio Florindo

National Institute of Geophysics and Volcanology

Gary Wilson

GNS Science

Maria Chiara Tartarello

Sapienza University of Rome

Claudio Mazzoli

University of Padua

Jacob Anderson

University of Otago

Valentina Romano

Sapienza University of Rome

Rachel Worthington

University of Otago

Sabina Bigi

Sapienza University of Rome

Raffaele Sassi

University of Padua

Giancarlo Ciotoli

National Research Council

Research Article

Keywords: Permafrost, soil gas survey, CO₂ output, McMurdo Dry Valleys, Antarctica

Posted Date: December 21st, 2021

DOI: <https://doi.org/10.21203/rs.3.rs-1154287/v1>

Abstract

McMurdo Dry Valleys comprise 10% of the ice-free soil surface areas in Antarctica. Permafrost stability plays an important role in C-cycle as it potentially stores considerable quantities of greenhouse gases. While the geomorphology of the Dry Valleys reflects a long history of changing climate conditions, comparison with the rapidly warming Northern polar region suggests that future climate and ecosystems may change more rapidly from permafrost degradation. In Austral summer 2019/2020 a comprehensive sampling of soil gases and CO₂ flux measurements was undertaken in the Taylor Valley, with the aims to identify potential presence of soil gases in the active layer. The results obtained show high concentrations of CH₄, CO₂, He and an increasing CO₂ flux rate. We identify the likely source of the gas to be from dissolved gases in deep brine moving from inland (potentially underneath the Antarctic Ice Sheet) to the coast at depth beneath the permafrost layer.

Highlights

- First extensive soil gas and CO₂ flux survey in Antarctica.
- Discovering of multigas anomalies zones.
- First CO₂ emission estimation in Taylor Valley.
- Abiotic origin identified for the CO₂.
- Baseline for future monitoring surveys.

1 Introduction

Permafrost is any ground (soil or rock and any ice and organic material inclusions) that remains completely frozen (0°C or colder) for at least two years¹. Its thaw and the microbial decomposition of previously frozen organic carbon is considered one of the most likely positive climate feedbacks from terrestrial ecosystems to the atmosphere in a gradually warming planet^{2,3}. Permafrost is present in both hemispheres at high latitudes and its temperature, thickness, and continuity are controlled by the geographic setting and, to a large extent, by the surface energy balance and thus vary strongly with latitude and it is present in both hemispheres at high latitudes⁴. Climate warming effects are going to impact these regions in the upcoming decades^{5,6} and all three types of permafrost below 1000 m elevation (dry, ice-cemented, and massive ice) may be susceptible to warming-related degradation depending on future emission pathways, for example through slumping of melt-lubricated sediments and surface ablation by sublimation-driven ice removal^{7,8}. Measurements of CO₂ and CH₄ soil concentrations and fluxes are essential to understand the C cycle in terrestrial ecosystems, although less is known about controls over CO₂ flux (φCO_2) in ecosystems lacking vascular vegetation, including polar deserts (such as the McMurdo Dry Valleys, thereafter MDV) and some hot deserts, where autotrophic inputs are low and abiotic factors tend to dominate in determining φCO_2 ⁹.

In the Arctic and boreal regions, permafrost is found in Greenland, Alaska, Canada, Northern Europe, Russia and China⁴, and represent 22% of the exposed land surface¹⁰. Studies carried out on permafrost soils in these ecosystems have shown how these areas store almost twice the carbon currently present in the

atmosphere^{4,11}. These regions are rich in frozen organic matter, that would lead to an increase of the production of CO₂ and CH₄ by microbial activities in case of thawing⁴. Furthermore, part of the released carbon could easily dissolve in water and, through solar radiation, produce CO₂ by the photomineralization process¹². Large methane deposits currently stored at high latitude regions are either frozen within permafrost or trapped below impermeable buffer zones¹³. Current and future warming will significantly affect polar and sub-polar regions triggering the melting of ice-bound sediments, releasing methane in to the Earth's atmosphere. Methane has a global warming potential 28 times higher than that of CO₂ on a 100-year time horizon¹⁴. It is therefore imperative to provide estimates of methane and other gases released from the high-latitude regions. In remote and scarcely monitored regions soil gas release can endure for decades or even centuries before being detected and quantified.

In the Southern Hemisphere, permafrost is found in the Sub-Antarctic islands, in the Antarctic Peninsula, at high elevations, and in the ice-free areas of the Antarctic region. Since Antarctica is much colder than the Arctic, it has limited organic content in soils⁴ and its ice-free area represents only 0.35% of the continent¹⁵, the degradation of permafrost has not been widely studied¹⁶. Nevertheless, if the temperature warms in Antarctica, the potential total amount of carbon contribution could be significant even at a fraction of the Northern Hemisphere. Also, the role of bacteria was in the past underestimated, and is potentially more important in Antarctica than previously believed. Indeed, microbial activity affects the amount of total organic carbon and is more susceptible to weak temperature variations⁴. The MDV are the largest ice-free regions in Antarctica¹⁷; their geomorphology reveals how the landscape is strongly controlled by climate processes¹⁸. Attempts to quantify CO₂ emissions in the Antarctic continent have been carried out in the MDV soils, highlighting that ϕ CO₂ is driven primarily by physical factors such as soil temperature and moisture, indicating that future climate change may alter the soil C cycle^{17,19-23}. The lack of mechanistic understanding makes it difficult to predict the contribution of soil ϕ CO₂ to the C-cycle due to climate change in the polar deserts of Antarctica. In the MDV, ϕ CO₂ has been used to characterize a variety of ecosystem processes and properties, including soil C turnover, the functional role of differing origins of organic matter supporting C cycling, and biotic distribution and activity²⁴⁻²⁸. In situ ϕ CO₂ in MDV soils is low and spatially variable²⁹, and it is therefore difficult to separate the biological processes (e.g. C-fixation) from physical factors (e.g. carbonate dissolution). Parsons et al.³⁰ hypothesized that in extreme desert environments, abiotic factors, like temperature gradients, parent material and soil water dynamics, may have the same magnitude of the biological processes influencing ϕ CO₂ rates; on the contrary, in lowest latitude ecosystems the physical ϕ CO₂ is negligible. Recent studies have revealed a diffuse subsurface brine system in the MDV area, occurring preferentially near the coast and under the surface sediments of the main valleys that could be carried from beneath the East Antarctic Ice Sheet³¹. The presence of this deep fluid circulation could also promote the uprising of geogenic gases. Soil gas measurements in the MDV were performed by Gregorich et al.²⁹ and by MacIntyre et al.²³ but both works provide few measurement points and were focused on biological process and temporal variability, respectively. In order to understand better the different mechanisms of production and migration of gas species in this environment, it is necessary to carry out a comprehensive survey. To date, no studies have been completed to investigate the soil gas spatial distribution in relation to possible fault and/or fracture systems and characterize seepage for both CO₂ and CH₄ in Antarctica. Soil gas geochemistry

is an alternative powerful approach that is widely used to detect diffusive/advective gas emissions and identify preferential migration pathways such as buried faults and fractured areas³²⁻³⁸. Permafrost is generally a barrier to the migration and leakage of endogenous gaseous species. However, the presence of faults, fractures and the thawing, could allow surface migration of anomalous concentrations of endogenous gaseous species. The challenge and the goal of this research is to understand the greenhouse gas potential that is trapped by MDV permafrost and, therefore, how much of these greenhouse gases would be released during thawing events. The rate of carbon release from permafrost soils is highly uncertain³⁹. More accurate estimates are crucial to predict the impact and timing of this carbon-cycle feedback effect, and thus how significant permafrost thaw will be for climate change this century and beyond. We report here the first large scale soil gas survey in Antarctica targeting the Taylor Valley as ideal locality for such type of study (Fig. 1). The sampling strategy was developed considering the logistical constraints and finalized to obtain the most representative results of the study area. Our work evaluates the magnitude and spatial distribution of the concentrations of some gases in the soil and of φCO_2 emission from permafrost and/or thawing shallow strata. The goal is to provide a first total CO_2 emission estimate for the lower Taylor Valley that can be used for future monitoring surveys and extrapolated more broadly across the continent.

2 Results

2.1 Soil gas composition and flux magnitude of the lower Taylor valley

Soil gas and flux surveys were carried out between 20 December 2019 and 25 January 2020. A total of 157 soil gas samples and 159 φCO_2 measurements were collected in an area of 21.6 km² with an average density of 7.3 samples/km² (Fig. 2).

The main statistics obtained for soil gas concentrations and φCO_2 are reported in Table 1. All gas species highlight broadly skewed distributions with the presence of few outliers (see SD and SK in Table 1). By comparing the mean and median values, the presence of outliers is particularly evident for H_2 and CH_4 (mean values > median values). The difference between the mean and median values also suggests a log-normal distribution for φCO_2 , CO_2 , CH_4 and H_2 .

To understand better the magnitude and the significance of the soil gas concentrations measured in Antarctica, calculated mean values are compared with the average concentrations of the same gaseous species present in the atmosphere, in the soil-atmosphere interface and in soil gases from the literature (Table 2). In Taylor Valley, O_2 , N_2 and Ne concentrations are broadly equal to their atmospheric concentration. In contrast, H_2 , CO_2 and CH_4 concentrations are higher than atmospheric concentrations. CO_2 mean concentration is twice as high as those normally measured in the soil gas. He concentrations highlight a mean value lower than the atmospheric concentration, and as evidenced by the 90% percentile, and only less than 10% of the total samples shows higher concentrations than the atmosphere.

2.2 Spatial distribution of soil gas concentrations and φCO_2 values

The soil gas and ϕCO_2 distributions were investigated to detect potential permafrost, or to identify the possible presence of faults and fractures, which may provide gas migration pathways. NPPs highlighted the following anomaly threshold values: 5.4 ppmv for He, 18.8 ppmv for Ne, 4 ppmv for H_2 , 9 ppmv for CH_4 , 0.5 vol% for CO_2 and $3 \text{ gm}^{-2}\text{d}^{-1}$ for ϕCO_2 . In Fig. 3A CH_4 spatial distribution shows higher values (up to 18,447 ppmv) in the NE and E sectors, and weak anomalies in the other sectors except for the central part of the study area where only background values occur. The contour map of CO_2 (Fig. 3B) shows diffuse anomalous values ($> 0.5 \text{ vol}\%$) to the S, SW and central sectors of the study area, while in the E sector background values dominate. Some weak anomalies are in close correspondence with those from CH_4 . The spatial distribution of ϕCO_2 is shown in Fig. 3C. Large anomaly zones are located in the NE and SE sectors, while higher anomalous values are in the central south part of the study area; weak anomalies are also present in the SW sector. H_2 distribution (Fig. 3D) shows small anomalous values scattered throughout the study area. However, some of the H_2 anomalies correspond with those observed for CH_4 and CO_2 . Regions with high concentrations of He (Fig. 3E) are distributed along N and S borders of the study area. Ne concentrations (Fig. 3F) largely increase together with He and are mostly located along the N edge of the study area.

3 Discussions

In the MDV, very limited data about soil gas concentrations are available (only CO_2 and CH_4), while for the most part they concern CO_2 and CH_4 flux measurements. In 2003-2005 austral summers, Gregorich et al.²⁹ measured up to 0.55 vol% of CO_2 and up to 5780 ppmv of CH_4 in Garwood valley. In January 2014, MacIntyre et al.²³ measured a maximum value of 0.044 vol% of CO_2 in the lower Taylor Valley, near Howard Glacier (Fig. 1). Both studies found CO_2 concentrations 1-2 orders of magnitude lower than the maximum value measured in this study (3.44 vol%, Table 1). The highest CH_4 value reported in Gregorich et al.²⁹ is in the same order of magnitude as found in this study, although more than three times lower than our maximum value (18,447 ppmv, Table 1). Both referenced studies, however, collected a limited number of measurements and focused on temporal variability rather than spatial variability. Worldwide, CO_2 and CH_4 soil gas data are numerous, and measured in different environments: in the Arctic Finnish Lapland, Voigt et al.⁴², measured CO_2 max value about 6 vol% and CH_4 max value about 300 ppmv. In Italy, CO_2 mean values of about 3 vol% for Tyrrhenian basins, 1.57 vol% for Apennine Intermontane plains and 1.09 vol% for foredeep basins, based on more than 10,000 samples⁴³.

In contrast, ϕCO_2 has been measured in Antarctica since 1994 (see Table 3). The ϕCO_2 measurements in this study are up to 3 orders of magnitude higher than previous studies, therefore, the highest measured in the MDV hereto. ϕCO_2 measurements in this work in Taylor Valley are on average comparable with the values measured in the Arctic^{25,44}, desert^{25,45} and alpine⁴⁶ areas and lower than other areas of the globe^{25,47} (Table 3).

The distribution of the positive anomalies for CH_4 , CO_2 , H_2 and ϕCO_2 are consistent in the NE, NW and S sectors of the study area, while He shows a good correlation with CO_2 and CH_4 anomalies in the S and N sectors, respectively. He detected in shallow soil is generally indicative of deep sources^{32,38}, and is typically

associated with CO₂ and CH₄ emissions that act as carrier gas for trace gases (i.e., He, Rn)^{35,48}. The source of these gas anomalies could be linked with shallow depth hypersaline fluids^{31,49} that during summer periods can release the dissolved gases after permafrost thawing. These gases can then easily migrate toward the surface through permeable layers, as well as local fractures and/or buried faults. These may act as preferential migration pathways thus resulting in the linear multigas anomalous zones observed in the study area^{35,37,48} (Fig. 4). Figure 4 shows gas anomalies aligned in ENE-WSW direction in the S and N sectors of the study area, respectively. At the northern boundary, the anomalous zone does not appear as continuous as that occurring in the southern boundary of the area because of the presence of the Commonwealth Glacier and related wetlands and streams (Fig. 2), that most likely prevent gas upwelling.

As for the southern sector, there are also two physical factors that may increase permafrost degradation: solar radiation and soil albedo. Solar radiation is more intense on North facing slopes than South facing slopes and in summer time soil temperatures increase in this sector^{18,50}. On the southern slope, south of Commonwealth Glacier is an area rich in dark basalt and anorthoclase phonolite⁵¹. Campbell et al.⁵² found the greatest heating on dark colored basalt soils. The combination of these phenomena may enhance the superficial degradation of the permafrost in the southern sector (i.e. where the major gaseous anomalies have been identified).

Regarding the origin of the atmospheric gases, the scatterplot of Fig. 5 shows the comparison between CO₂, O₂, and N₂ concentrations. The linear trend of the samples in the graph shows the existence of a dilution process of atmospheric gases (N₂ and O₂) by CO₂. This effect leads to exclude a biological or atmospheric contribution to the soil system, but may be linked to a different intake of CO₂, for example, geological and/or abiotic contributions⁵³. These hypotheses can be confirmed only with isotope analyses of gas samples. In the literature, the origin of CO₂ in Antarctic soils is suggested to be linked to biological activity, favored by soil alkalinity and by shallow abiotic processes (CO₂ solubility), soil moisture content and soil temperature variations^{19,21,23,29,30}. Shanhun et al.⁹ and Risk et al.⁵⁴ suggested an abiotic origin of CO₂ based on the isotopic analyses, reporting very high positive $\delta^{13}C_{CO_2}$ values that cannot be explained by normal microbial activity. We suggest that the measured high anomaly values, originate from the subsurface brine system^{31,49}, and are linked to permafrost cap discontinuities at the edges of the valley (fractures or buried local faults). The spatial distribution of these anomalous zone could also be locally influenced by shallow permafrost thawing.

Although the samples were collected at shallow depths (i.e. permafrost is often reached at 30 cm depth) and are potentially affected by atmospheric gas dilution^{55,56}, the anomalous values of He, CH₄, CO₂ and $\delta^{13}C_{CO_2}$ cannot entirely be explained by biological activity and/or superficial physical processes. Another aspect concerns the presence of soil moisture which prevents both sampling and gas rising^{55,56}. In Taylor Valley, the wetlands represent an area where water permeates the pores of the soil but does not emerge on the surface. Within these areas (Fig. 2) we managed to complete some sampling stations, however it should be noted that the gas concentrations are certainly underestimated compared to those conducted in dry and ventilated soil conditions. In these areas, of about 2.1 km² (equal to 10% of the total area) 16 soil gas samples and $\delta^{13}C_{CO_2}$ were collected. Statistical analyses (Table S1) confirm the low values in these areas.

Figure 6 shows the ranging and average values of ϕCO_2 measured over time in Antarctica. It should be noted that the reported measurements were conducted using various methods and in different environments, e.g. there are measurements on dry soil, near and from lakes and from the Ross Sea. Data collected in Dec 2019 - Jan 2020 from Taylor Valley show that the average value is in the same order of magnitude of those reported from the Garwood Valley²⁹. The maximum values measured in this work, instead, is at least one order of magnitude higher than those previously reported. Focusing on Taylor Valley, various measurements have been carried out over the years, both in the soils^{9,25} and around the three lakes³⁰. The comparison of these data shows that our values are two orders of magnitude greater than those previously measured.

The total CO_2 gas emission rates over the surveyed area ($A = 21.6 \text{ km}^2$) have been computed following a statistical approach (see 2.3 Statistical and geostatistical analysis) and, the calculated average CO_2 output is 14.95 t d^{-1} (Table S2). The calculated total CO_2 emission considering the three summer months, is about 1,345.5 t. This value is also considered as the total annual CO_2 emitted, providing a conservative estimate for the warmest months expecting much lower emissions during the rest of the year. Then, the estimated emission factor in the study area is $62.3 \text{ t km}^{-2} \text{ y}^{-1}$. Comparing this value, for example, with those estimated for the central Apennines in Italy, ranging from 350 to $1,050 \text{ t km}^{-2} \text{ y}^{-1}$ ⁽⁵⁷⁾, it is evident that the fluxes reported herein are remarkably lower, even compared with others reported worldwide⁵⁸. This discrepancy is due to both climate/environmental differences and organic content and biological activity usually present in the soils of the other continents. Although our emission values are low, forecasting that ice-free regions in Antarctica are likely to expand with gradual warming, this amount will tend to increase and should be counted in the global CO_2 budget estimations.

To conclude, we provide the first spatial distribution maps of soil gas concentrations and ϕCO_2 in a large area ($> 20 \text{ km}^2$) of the Taylor Valley, Antarctica. The calculated CO_2 emission output during the summer period is 1,345.5 t. Our results emphasize that extensive surveys are necessary to properly evaluate greenhouse gas (GHG) emissions in regions with permafrost. We also established the first extensive baseline maps that can be used to compare and monitor soil gas concentrations and CO_2 emissions in the region. The collected data identified areas characterized by multigas anomalies where permafrost partial melting may occur during the summer period and where fluids migrate to the surface through structures/fractures aligned with the main direction of the valley. We suggest that the gases originate from the subsurface brine system that is rich in dissolved gasses. The superficial melting of the permafrost and the presence of permeable zones inside it, allowed these gases to migrate to the surface.

4 Methods

4.1. Site description and sampling strategy

The MDV feature a mosaic of ice-covered lakes, ponds, ephemeral streams, valley glaciers and glacial, fluvial, lacustrine and aeolian sediments. Mean annual air temperature in the valleys is -17°C , and annual precipitation (snow water equivalent) spans 3–50 mm⁵⁹, making the MDV a cold, polar desert⁶⁰. Continuous permafrost, by definition, is a regional land surface with temperatures below 0°C on interannual timescales,

and underlies 90–100% of the MDV. This permafrost is predominantly ice-cemented (ranging from ice-saturated to weakly cemented), although overlying “dry-frozen” (ice-free) permafrost is common in the upper ~1 m along valley walls²⁰. Massive buried ice (ground ice) is common in the MDV and has been mapped in the Quartermain Range, in Victoria Valley, and in extensive ice-cored Ross Sea drift deposits emplaced during the last glacial maximum^{20,61,62}. Taylor Valley (77°37' S, 163°15' E) is the southernmost of the three large Dry Valleys in the Transantarctic Mountains and extends WSW-ENE for ~29 km from Taylor Glacier to the McMurdo Sound (Fig. 1). Our study area is located in the eastern sector of the valley and extends for 6 km to the east of the Lake Fryxell bordering the southern part of the Commonwealth glacier (Fig. 2). The area is characterized by hummocky moraines, lacustrine deposits, and outwash fans where ephemeral streams and water tracks are active during summer. Recent studies also documented the presence of shallow underground brine systems^{31,49}.

4.2 Soil gas and ϕCO_2 measurements

Typically soil gas survey samples are collected from the soil pore air by pounding a steel probe in the soil at a depth of about 0.6-0.8 m^{55,56}. However, in the presence of a shallow permafrost cap, our soil gas samples were collected at the bottom of the active layer that was present to depths ranging between 0.15 to 0.5 m (average depth of about 0.3 m). Elemental gas composition was then analyzed at Scott Base (at Pram Point on Ross Island) two weeks after collection to determine the concentrations of He, Ne, H₂, O₂, N₂, CH₄, CO₂. We used a MicroGC Varian 4900 CP, equipped with two Thermal Conductivity Detectors (TCD), responding to the difference in thermal conductivity between the carrier gas (Ar) and the sample components.

ϕCO_2 measurements were measured directly in the field by using a West System™ portable fluxmeter equipped with an IR Spectrometry detector (LICOR–LI820), with high accuracy in the range from 0 up to 600 mol m⁻² d⁻¹ (0 - 26400 g m⁻² d⁻¹).

The concentration change over time is converted into CO₂ flux in g m⁻² d⁻¹ considering the pressure and temperature variations measured during the day, together with volume (0.0028 m³) and surface (0.0306 m²) of the accumulation chamber, using the formula:

$$(\phi\text{CO}_2 * (86400 * P * (V/A)) / (1000000 * R * T)) * M$$

where ϕCO_2 is the soil flux expressed in ppm/sec; P is the pressure in mbar; V is volume (m³) and A is surface area (m²) of the accumulation chamber; T is the temperature in K; M is molecular weight; R = 0.08314472 in bar L (K mol)⁻¹ that is used to calculate the volume in L of an ideal gas from its temperature in K, pressure in bar and mole number.

4.3 Statistical and geostatistical analysis.

Exploratory Data Analysis (EDA) (numerical and graphical techniques) was applied to elaborate soil gas data in terms of main statistical parameters, distribution type, background, and anomalous values. Normal probability plots (NPP) were interpreted according to the Sinclair method⁶³ in order to distinguish different populations and statistical anomaly threshold values for each gas species (see Fig. S1). Subsequently,

geostatistical analysis (e.g., variogram analysis and kriging^{35,43}) was applied to construct contour maps to represent the spatial distribution of gas concentrations in the surveyed area. Furthermore, φCO_2 measurements were used to estimate the total output of CO_2 emission from the soil to the atmosphere in the investigated area⁶⁴. This emission rate (expressed in t d^{-1}) was calculated by multiplying the average flux value of each population recognized in the NPP by the respective area estimated in the contour map. The contributions of the different populations (excluding background values) were then summed to obtain the total φCO_2 (see table S2).

Declarations

Acknowledgments

This work is part of the PNRA 2018 SENECA project and was financially supported by CNR (PNRA 2018 n° 00253 linea D, prot.73633/2019, SENECA PROJECT: Source and origin of greenhouses gases in Antarctica). All the data were collected during the XXXV Italian expedition in Antarctica, we thank PNRA and UTA ENEA for the logistic support. SENECA is a joint project of international cooperation between Italy, New Zealand and Norway. We thank the Antarctica New Zealand for the scientific, logistical and technical support and the Scott Base personnel for hosting our research team. We acknowledge the support of the Research Council of Norway (NFR) through the HOTMUD project number 288299 and its Centres of Excellence funding scheme, project number 223272 (CEED).

Authors Contributions

L.R. and A.S. led the conceptual development of the study and designed the project. L.R., A.S., A.M., F.F., G.W., C.M., M.C.T., J.T.H.A., R.W. and V.R. data collection. A.S. and M.C.T. analyzed the data. L.R., A.S., G.C. and A.M. interpreted the data. L.R., A.S. and G.C. wrote original manuscript. L.R., A.S., A.M., J.T.H.A, F.F., G.W., R.S. and S.B. drafted the paper. L.R. Principal Investigator of the SENECA project.

Competing interests

The authors declare no competing financial interests.

References

1. Van Everdingen, R. Multi-language glossary of permafrost and related ground-ice terms. National Snow and Ice Data Center/World Data Center for Glaciology, Boulder, CO. <http://nsidc.org/fgdc/glossary> (2005).
2. Schuur, E. A. et al. Climate change and the permafrost carbon feedback. *Nature***520**, 171-179 doi:10.1038/nature14338 (2015).
3. Xue, K., et al. Tundra soil carbon is vulnerable to rapid microbial decomposition under climate warming. *Clim. Change***6**, 595-600 (2016).
4. Schuur, E. A. et al. Vulnerability of permafrost carbon to climate change: Implications for the global carbon cycle. *BioScience***58**, 701-714 (2008).

5. Shindell, D.T., Schmidt, G.A. Southern hemisphere climate response to ozone changes and greenhouse gas increase. *Res. Lett.* **31**, L18209 (2004).
6. Chapman, W.L., Walsh, J.E. A synthesis of Antarctic temperatures. *Clim.***20**, 4096–4117 (2007).
7. Hagedorn, B., Sletten, R.S., Hallet, B. Sublimation and ice condensation in hyperarid soils: modeling results using field data from Victoria Valley, Antarctica. *Geophys. Res.* **112**, F03017 (2007).
8. Swanger, K.M., Marchant, D.R. Sensitivity of ice-cemented Antarctic soils to greenhouse-induced thawing: are terrestrial archives at risk? *Earth Planet. Sci. Lett.* **259**, 347–359 (2007).
9. Shanahun, F. L., Almond, P. C., Clough, T. J., & Smith, C. M. Abiotic processes dominate CO₂ fluxes in Antarctic soils. *Soil Biol. Biochem.***53**, 99-111 (2012).
10. Zhang, T., Barry, R. G., Knowles, K., Heginbottom, J. A., & Brown, J. Statistics and characteristics of permafrost and ground-ice distribution in the Northern Hemisphere. *Polar Geogr.***23**, 132-154 (1999).
11. Schuur, E.A.G., Vogel, J.G., Crummer, K.G., Lee, H., Sickman, J.O., Osterkamp, T.E. The effect of permafrost thaw on old carbon release and net carbon exchange from tundra. *Nature***459**, 556–559 (2009).
12. Cory, R.M., Ward, C.P., Crump, B.C., & Kling, G.W. Sunlight controls water column processing of carbon in arctic fresh waters. *Science***345**, 925–928 (2014).
13. Anthony, K. M. W., Anthony, P., Grosse, G., & Chanton, J. Geologic methane seeps along boundaries of Arctic permafrost thaw and melting glaciers. *Geosci.* **5**, 419-426 (2012).
14. Ciais, P. et al. Carbon and Other Biogeochemical Cycles. In: *Climate Change 2013: The Physical Science Basis*. Contribution of Working Group I to the Fifth Assessment Report of the Intergovernmental Panel on Climate Change. Eds: Stocker, T.F., D. Qin, G.-K. Plattner, M. Tignor, S.K. Allen, J. Boschung, A. Nauels, Y. Xia, V. Bex and P.M. Midgley (Cambridge University Press, Cambridge, United Kingdom and New York, NY, USA, pp. 465–570, 2013).
15. Campbell, I.B., & Claridge, G.G. Antarctic permafrost soils. In *Permafrost soils*. (Springer, Berlin, Heidelberg, pp. 17-31, 2009).
16. Levy, J. et al. Accelerated thermokarst formation in the McMurdo Dry Valleys, Antarctica. *Rep.***3**, 2269 (2013).
17. Gilichinsky, D.A. et al. Microbial Populations in Antarctic Permafrost: Biodiversity, State, Age, and Implication for Astrobiology. *Astrobiology***7**, 275-311 (2007).
18. Fountain, A.G., Levy, J.S., Gooseff, M.N., & Van Horn, D. The McMurdo Dry Valleys: a landscape on the threshold of change. *Geomorphology***225**, 25-35 (2014).
19. Elberling, B., Gregorich, E.G., Hopkins, D.W., Sparrow, A.D., Novis, P., Greenfield, L.G. Distribution and dynamics of soil organic matter in an Antarctic dry valley. *Soil Biol. Biochem.***38**, 3095-3106 (2006).
20. Bockheim, J.G., Campbell, I.B., McLeod, M. Permafrost distribution and active-layer depths in the McMurdo Dry Valleys, Antarctica. *Periglac. Process***18**, 217–227 (2007).
21. Ball, B.A., Virginia, R.A., Barrett, J.E., Parsons, A.N., Wall, A.H. Interactions between physical and biotic factors influence CO₂ flux in Antarctic dry valley soils. *Soil Biol. Biochem.* **41**, 1510-1517 (2009).
22. Faucher, B., Lacelle, D., Davila, A., Pollard, W., Fisher, D., and McKay, C.P. Physicochemical and Biological Controls on Carbon and Nitrogen in Permafrost from an Ultraxerous Environment, McMurdo Dry Valleys of Antarctica. *Geophys. Res. Biogeosci.***122**, 2593–2604 (2017).

23. MacIntyre, C., Risk, D., Lee, C.K., & Cary, S.C. Processes driving soil CO₂ temporal variability in Antarctic Dry Valleys. *Geoderma***337**, 871-879 (2019).
24. Virginia, R.A., Wall, D.H. How Soils Structure Communities in the Antarctic Dry Valleys. *Bioscience***49**, 973–983 (1999)
25. Burkins, M.B., Virginia, R.A., Wall, D.H. Organic carbon cycling in Taylor Valley, Antarctica: quantifying soil reservoirs and soil respiration. *Chang. Biol.* **7**, 113–125 (2001).
26. Adams, B.J. et al. Diversity and distribution of Victoria Land biota. *Soil Biol. Biochem.* **38**, 3003–3018 (2006).
27. Barrett, J.E., Virginia, R.A., Wall, D.H., Cary, S.C., Adams, B.J., Hacker, A.L., Aislabie, J.M. Co-variation in soil biodiversity and biogeochemistry in northern and southern Victoria Land, Antarctica. *Sci.* **18**, 535 (2006).
28. Hopkins, D.W. et al. Carbon, nitrogen and temperature controls on microbial activity in soils from an Antarctic dry valley. *Soil Biol. Biochem.* **38**, 3130–3140 (2006).
29. Gregorich, E.G. et al. Emission of CO₂, CH₄ and N₂O from lakeshore soils in an Antarctic dry valley. *Soil Biol. Biochem.***38**, 3120–3129 (2006).
30. Parsons, A.N., Barrett, J.E., Wall, D.H., Virginia, R.A. Soil Carbon Dioxide Flux in Antarctic Dry Valley Ecosystems. *Ecosystems***7**, 286–295 (2004).
31. Mikucki, J. A. et al. Deep groundwater and potential subsurface habitats beneath an Antarctic dry valley. *Commun.***6**, 6831 doi: 10.1038/ncomms7831 (2015).
32. Baubron, J.-C., Rigo, A., Toutain, J.-P. Soil gas profiles as a tool to characterize active tectonic areas: The Jaut Pass example (Pyrenees, France). *Earth Planet. Sci. Lett.***196**, 69–81 (2002).
33. Bigi, S. et al. Mantle-derived CO₂ migration along active faults within an extensional basin margin (Fiumicino, Rome, Italy). *Tectonophysics***637**, 137-149 (2014).
34. Ciotoli, G., Etiope, G., Marra, F., Florindo, F., Giraudi, C., & Ruggiero, L. Tiber delta CO₂-CH₄ degassing: a possible hybrid, tectonically active sediment-hosted geothermal system near Rome. *Geophys. Res. Solid Earth***121**, 48-69 (2016).
35. Ascione, A. et al. Assessing mantle versus crustal sources for non-volcanic degassing along fault zones in the actively extending southern Apennines mountain belt (Italy). *GSA Bulletin* Data Repository item 2018150. <https://doi.org/10.1130/B31869.1> (2018).
36. Sciarra, A., Mazzini, A., Inguaggaito, S., Vita, F., Lupi, M., Hadi, S. Radon and carbon gas anomalies along the Watukosek Fault System and Lusi mud eruption, Indonesia. *Pet. Geol.***90**, 77-90, <https://doi.org/10.1016/j.marpetgeo.2017.09.031>, (2018).
37. Sciarra, A., Cantucci, B., Ricci, T., Tomonaga, Y., & Mazzini, A. Geochemical characterization of the Nirano mud volcano, Italy. *Geochem.***102**, 77-87 <https://doi.org/10.1016/j.apgeochem.2019.01.006>, (2019).
38. Sciarra, A. et al. Geochemical and geoelectrical characterization of the Terre Calde di Medolla (Emilia-Romagna, northern Italy) and relations with 2012 seismic sequence. *Geochem. Explor.***221**<https://doi.org/10.1016/j.gexplo.2020.106678>, (2021).
39. Burke, E.J., et al. Quantifying uncertainties of permafrost carbon–climate feedbacks. *Biogeosciences***14**, 3051-3066 (2017).

40. Rose A.W., Hawkes H.W., Webb J.S. *Geochemistry in mineral exploration*. Second Edition, (Academic Press, London, 657 pp, 1979).
41. Holland, P.W., & Emerson, D.E. The global helium-4 content of near-surface atmospheric air. In *Geochemistry of gaseous elements and compounds*, pp. 97-109, (1990).
42. Voigt, C., et al. Ecosystem carbon response of an Arctic peatland to simulated permafrost thaw. *Change Biol.***25**, 1746-1764 (2019).
43. Ciotoli, G., et al. Soil gas distribution in the main coseismic surface rupture zone of the 1980, Ms= 6.9, Irpinia earthquake (southern Italy). *Geophys. Res. Solid Earth***119**, 2440-2461 (2014).
44. Turetsky, M.R., Wieder, R.K., & Vitt, D.H. Boreal peatland C fluxes under varying permafrost regimes. *Soil Biol. Biochem.***34**, 907-912 (2002).
45. Mazzini, A., Lupi, M., Sciarra, A., Hammed, M., Schmidt, S.T. and Suessenberger, A. Concentric Structures and Hydrothermal Venting in the Western Desert, Egypt. *Earth Sci.* **7**, 266, doi: 10.3389/feart.2019.00266, (2019).
46. Sommerfeld, R.A., Mosier, A.R., & Musselman, R.C. CO₂, CH₄ and N₂O flux through a Wyoming snowpack and implications for global budgets. *Nature***361**, 140-142 (1993).
47. Oechel, W.C., Hastings, S.J., Vourlitis, G., Jenkins, M., Riechers, G., & Grulke, N. Recent change of Arctic tundra ecosystems from a net carbon dioxide sink to a source. *Nature***361**, 520-523 (1993).
48. Ciotoli, G., Lombardi, S., & Annunziatellis, A. Geostatistical analysis of soil gas data in a high seismic intermontane basin: Fucino Plain, central Italy. *Geophys. Res. Solid Earth***112**(B5) (2007).
49. Foley, N. et al. Evidence for pathways of concentrated submarine groundwater discharge in east Antarctica from helicopter-borne electrical resistivity measurements. *Hydrology***6**, 54 <https://doi.org/10.3390/hydrology6020054>, (2019).
50. Lacelle, D. et al. Solar radiation and air and ground temperature relations in the cold and hyper-arid Quartermain Mountains, McMurdo Dry Valleys of Antarctica. *Periglac. Process.***27**, 163-176 (2016).
51. Murrell, B. Cenozoic stratigraphy in Lower Taylor Valley, Antarctica. *Z. J. Geol. Geophys.***16**, 225-242 (1973).
52. Campbell, I.B., Claridge, G.G.C., Campbell, D.I., & Balks, M.R. Permafrost properties in the McMurdo Sound Dry Valley Region of Antarctica. Proceedings In Seventh International Conference on Permafrost, Yellowknife (Canada), *Collection Nordicana***55**, 121-126 (1998).
53. Romanak, K.D., Bennett, P.C., Yang, C., & Hovorka, S.D. Process-based approach to CO₂ leakage detection by vadose zone gas monitoring at geologic CO₂ storage sites. *Res. Lett.***39**, (2012).
54. Risk, D., Lee, C. K., MacIntyre, C., & Cary, S. C. First year-round record of Antarctic Dry Valley soil CO₂. *Soil Biol. Biochem.* **66**, 193-196 (2013).
55. Hinkle, M. E. Environmental conditions affecting concentrations of He, CO₂, O₂ and N₂ in soil gases. *Geochem.***9**, 53-63 (1994).
56. Beaubien, S.E. et al. The importance of baseline surveys of near-surface gas geochemistry for CCS monitoring, as shown from onshore case studies in northern and southern Europe. *Oil Gas Sci. Technol.* **70**, 615-633 (2015).

57. Chiodini, G., Frondini, F., Cardellini, C., Parello, F., & Peruzzi, L. Rate of diffuse carbon dioxide Earth degassing estimated from carbon balance of regional aquifers: The case of central Apennine, Italy. *Geophys. Res. Solid Earth***105**, 8423-8434 (2000).
58. Mörner, N. A., & Etiope, G. Carbon degassing from the lithosphere. *Planet. Change***33**, 185-203 (2002).
59. Fountain, A.G., Nylén, T.H., Monaghan, A., Basagic, H.J., Bromwich, D. Snow in the McMurdo Dry Valleys, Antarctica. *J. Climatol.***30**, 633–642 (2010).
60. Monaghan, A.J., Bromwich, D.H., Powers, J.G., Manning, K.W. The Climate of the McMurdo, Antarctica, Region as Represented by One Year of Forecasts from the Antarctic Mesoscale Prediction System. *Climate***18**, 1174–1189 (2005).
61. Hall, B.L., Denton, G.H. Radiocarbon chronology of Ross Sea drift, eastern Taylor Valley, Antarctica: evidence for a grounded ice sheet in the Ross Sea at the last glacial maximum. *Ann.***82A**, 305–336 (2000).
62. Swanger, K.M., Marchant, D.R., Kowalewski, D.E., Head, J.W. Viscous flow lobes in central Taylor Valley, Antarctica: origin as remnant buried glacial ice. *Geomorphology***120**, 174–185 (2010).
63. Sinclair, A. J. A fundamental approach to threshold estimation in exploration geochemistry: probability plots revisited. *Geochem. Explor.***41**, 1-22 (1991).
64. Chiodini, G., & Frondini, F. Carbon dioxide degassing from the Albani Hills volcanic region, Central Italy. *Geol.* **177**, 67-83 (2001).
65. Arrigo, K.R., & Van Dijken, G.L. Interannual variation in air-sea CO₂ flux in the Ross Sea, Antarctica: A model analysis. *Geophys. Res.: Oceans*, **112** (2007)
66. Zhu, R., et al. Carbon dioxide and methane fluxes in the littoral zones of two lakes, east Antarctica. *Environ.***44**, 304-311 (2010).
67. Moore, T.R., & Knowles, R. Methane and carbon dioxide evolution from subarctic fens. *J. Soil Sci.***67**, 77-81(1987).
68. Vitt, D.H., & Chee, W.L. The relationships of vegetation to surface water chemistry and peat chemistry in fens of Alberta, Canada. *Vegetatio***89**, 87-106 <https://doi.org/10.1007/BF00032163>, (1990).
69. Shannon, G., Heyes, A., Moore, T. Carbon dioxide and methane fluxes from drained peat soils, southern Quebec. *Biogeochem. Cycles***7**, 247-257 (1993).
70. Oertel, C., Matschullat, J., Zurba, K., Zimmermann, F., & Erasmi, S. Greenhouse gas emissions from soils— A review. *Geochemistry***76**, 327-352, <https://doi.org/10.1016/j.chemer.2016.04.002>, (2016).

Tables

Table 1. Descriptive statistics of He, Ne, H₂, O₂, N₂, CH₄, CO₂ soil gas concentration and φCO₂ measurements carried out in the Lower Taylor Valley.

	N	Mean	Median	Min	Max	LQ	UQ	P10%	P90%	SD	SK
He (ppmv)	157	5.08	5.06	4.20	6.49	5.0	5.13	4.74	5.24	0.30	1.77
Ne (ppmv)	157	17.61	17.48	15.23	22.12	17.15	17.84	16.98	18.39	0.83	2.15
H ₂ (ppmv)	157	3.57	1.79	0.15	36.95	1.02	2.73	0.65	9.51	5.60	3.59
O ₂ (vol%)	157	20.82	20.88	19.52	21.09	20.75	20.94	20.59	20.99	0.20	-3.07
N ₂ (vol%)	157	76.18	76.25	74.23	77.19	75.95	76.54	75.50	76.77	0.53	-1.03
CH ₄ (ppmv)	157	220.3	3.7	1.8	18447	3.2	4.4	2.9	25.3	1553	10.7
CO ₂ (vol%)	157	0.53	0.20	0.04	3.44	0.06	0.78	0.05	1.52	0.69	2.01
φCO ₂ (g m ⁻² d ⁻¹)	159	1.73	1.20	-0.74	11.36	0.74	2.08	0.42	4.11	1.63	2.22

N: number of observations; LQ: lower quartile; UQ: upper quartile; P10%: percentile 10%; P90%: percentile 90%; SD: standard deviation; SK: skewness.

Table 2. Comparison of gas content measured in the Lower Taylor Valley and air composition at different layers in the surficial environment. Typical average values of soil gas concentration of Ne, O₂, N₂, H₂O, Ar, CO₂, He, CH₄, and H₂ in the Taylor Valley (this work), atmospheric air, atmosphere-soil interface and soil gas.

	Taylor Valley (this work)	Atmospheric air	Atmosphere-soil interface	Soil gas
N ₂ (vol%)	76.18	78.08	78.08	79.2
O ₂ (vol%)	20.82	20.95	20.94	20.6
H ₂ O (%)	-	0.1 – 4	na	na
Ar (%)	-	0.93	0.93	na
CO ₂ (vol%)	0.53	0.035	0.031	0.25
Ne (ppmv)	17.61	18	na	na
He (ppmv)	5.08	5.24	5.22*	na
CH ₄ (ppmv)	220.3	1.4	1.4	na
H ₂ (ppmv)	3.57	0.5	0.5	na

Modified from Rose et al.⁴⁰; *Holland & Emerson⁴¹

Table 3. Summary table of ϕCO_2 measured in different terrestrial environments. Soil emission rates in $\text{g m}^{-2} \text{d}^{-1}$ from Antarctic, Arctic, and other ecosystems (e.g., Alpine and sub-alpine, Mediterranean, desert and tropical climates).

Study site	Date	CO ₂ rate (g m ⁻² d ⁻¹)
Antarctic		
Taylor Valley ²⁵	1994-1997	0,1
Ross Sea ⁶⁵	1997-2003	-0.35 – -0.02
Lake Fryxell, Taylor Valley ³⁰	2001-2002	-0.3 – 0.57
Lake Hoare, Taylor Valley ³⁰	2001-2002	-0.38 – 0.42
Lake Bonney, Taylor Valley ³⁰	2001-2002	0.004 – 0.08
Upper moraine; Garwood Valley ¹⁹	2003	0.0005
Delta; Garwood Valley ¹⁹	2003	0.0006
Sand dune; Garwood Valley ¹⁹	2003	0.00045
Lower moraine; Garwood Valley ¹⁹	2003	0.0009
Polygons; Garwood Valley ¹⁹	2003	0.0007
Hill slope; Garwood Valley ¹⁹	2003	0.0008
Stream edge; Garwood Valley ¹⁹	2003	0.0024
Lake edge; Garwood Valley ¹⁹	2003	0.0137
Garwood Valley ²⁹	2003	0.9504
Garwood Valley ²⁹	2005	1.59
Lake Mochou ⁶⁶	2007-2008	-1.70
Lake Tuanjie ⁶⁶	2007-2008	-0.89
Taylor Valley ⁹	2008-2009 h13:00-15:00	0.097
Taylor Valley ⁹	2008-2009 h06:00-08:00	-0.09
Hidden Valley ⁵⁴	2011	0.02 – 1.56
<i>Taylor Valley (this work)</i>	<i>2019-2020</i>	<i>1.73</i>
Arctic		
Subarctic fens, Canada ⁶⁷	-	0.09 – 1.28
Bog, Canada ⁶⁸	-	0.05
Poor fen, Canada ⁶⁸	-	0.17

Drained swamp peatlands, Canada ⁶⁹	-	0 – 0.016
Toolik Lake, Alaska ⁴⁷	-	0.15 – 0.78
Arctic tundra ²⁵	-	1.59
Boreal peatland, Canada ⁴⁴	-	0.08
Other ecosystems		
Sub-alpine snowpack ⁴⁶	-	2.046
Alpine snowpack ⁴⁶	-	0.693
Desert scrub soil ²⁵	-	0.59
Deciduous forest soil ²⁵	-	2.5
Tropical soil ²⁵	-	3.34
Temperate ⁷⁰	-	1.9 - 30.41
Mediterranean ⁷⁰	-	1.9 - 10.26
Subtropical ⁷⁰	-	2.66 - 4.94
Rocky Desert ⁴⁵	-	6.17

Figures

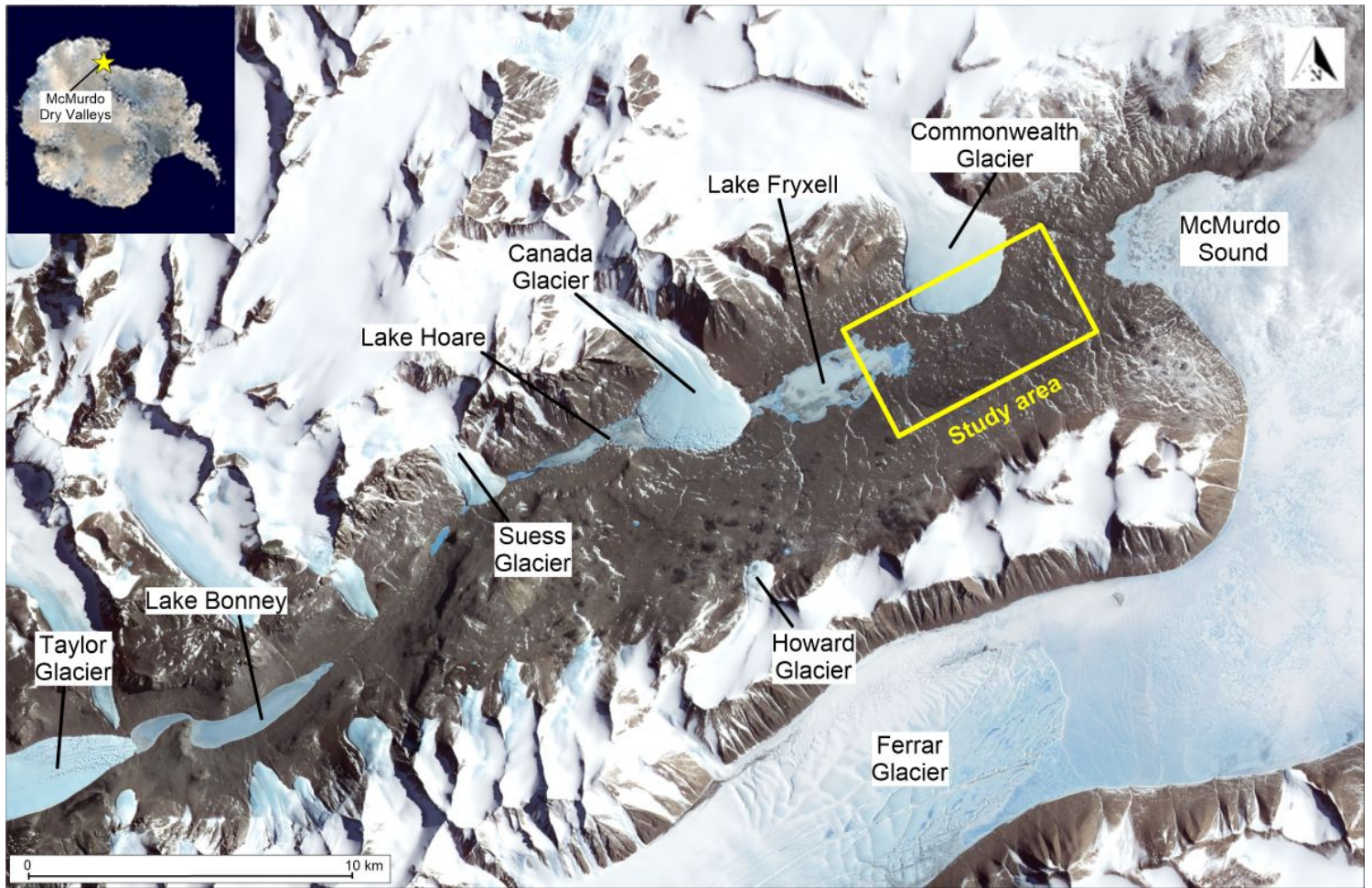


Figure 1

Location of the study area (yellow square) in the Taylor Valley, McMurdo Dry Valleys, Victoria land, West Antarctica. The inferred area is located among the Lake Fryxell, the Commonwealth Glacier and the McMurdo Sound. The inset indicates the location of the McMurdo Dry valleys. (credit: NASA).

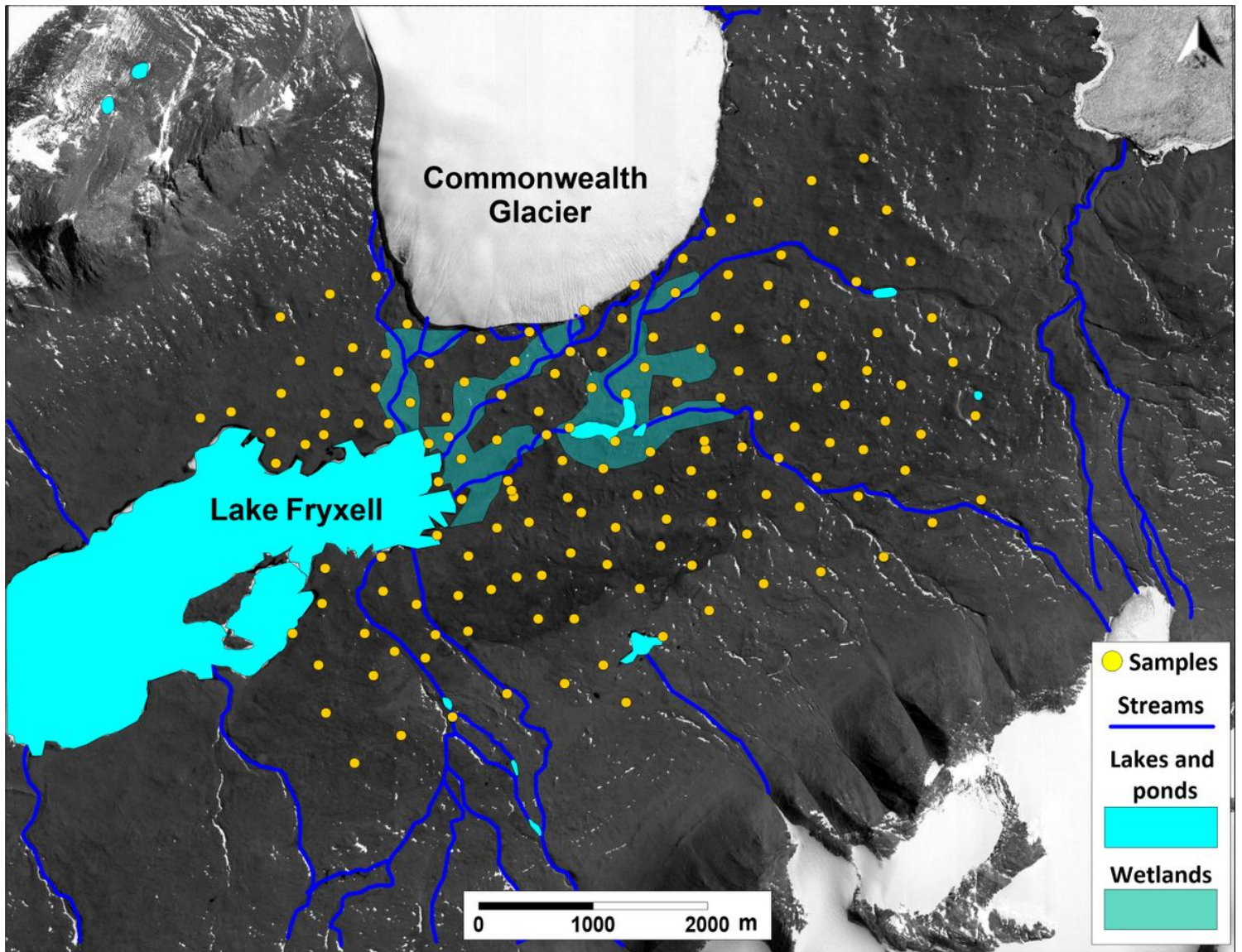


Figure 2

Location of soil gas and ϕCO_2 measurement points (yellow dots), of lakes and ponds (cyan areas), streams (blue lines) and wetlands (sea green areas) within Lower Taylor Valley.

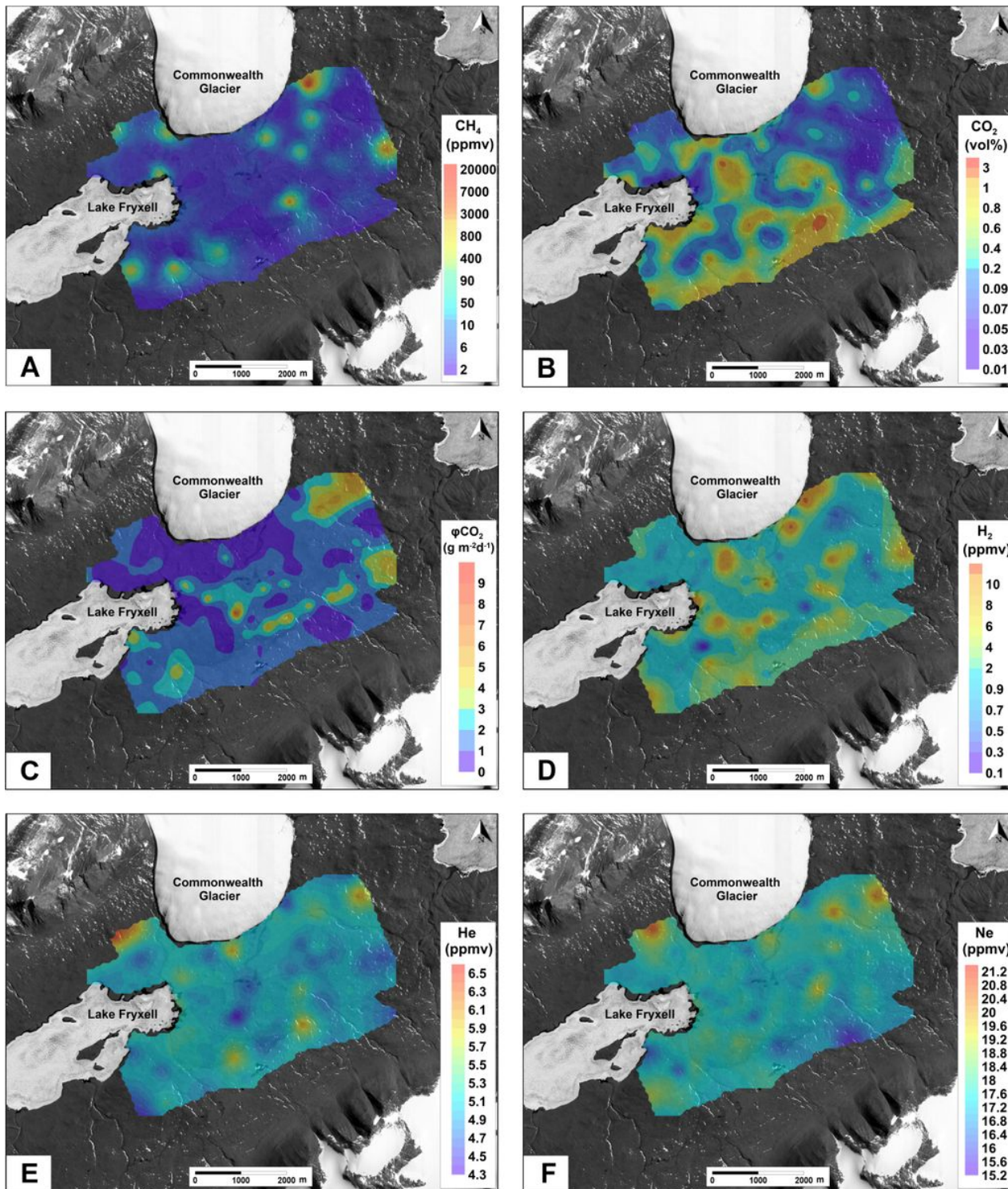


Figure 3

Contour maps of the analyzed gas species and the ϕCO_2 . The figure shows the spatial distribution of CH_4 concentrations (A), CO_2 concentrations (B), ϕCO_2 (C), H_2 concentrations (D), He concentrations (E) and Ne concentrations (F) obtained by means of geostatistical analysis, in the Lower Taylor Valley.

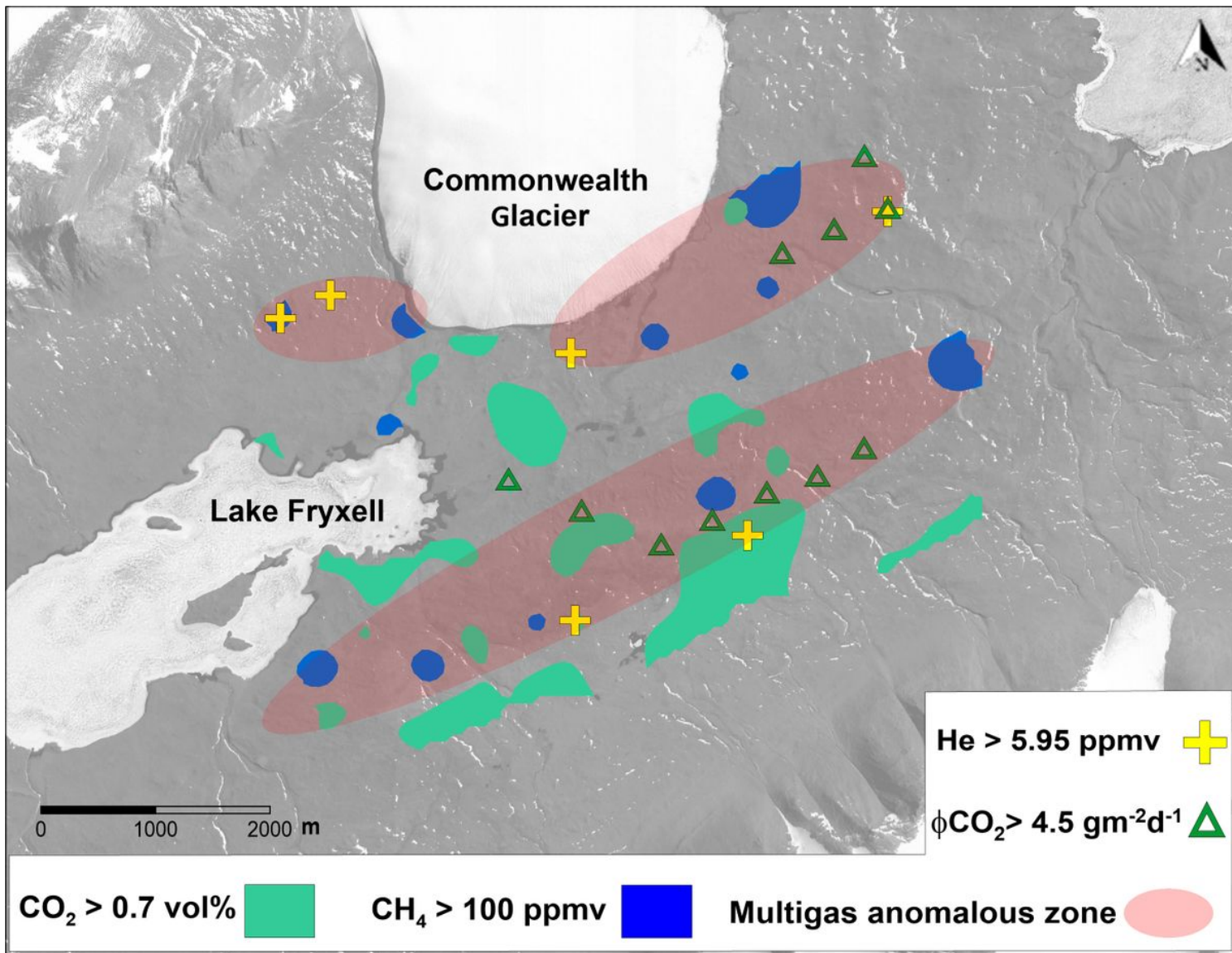


Figure 4

The map shows contour areas of CO₂ (green) and CH₄ (blue) concentrations higher than 0.7 vol% and 100 ppmv, respectively, samples with He higher than 5.95 ppmv (yellow crosses), φCO₂ higher than 4.5 g m⁻²d⁻¹ (green triangles). The map also shows, in pink ellipsoid, the multigas anomalous zones recognized.

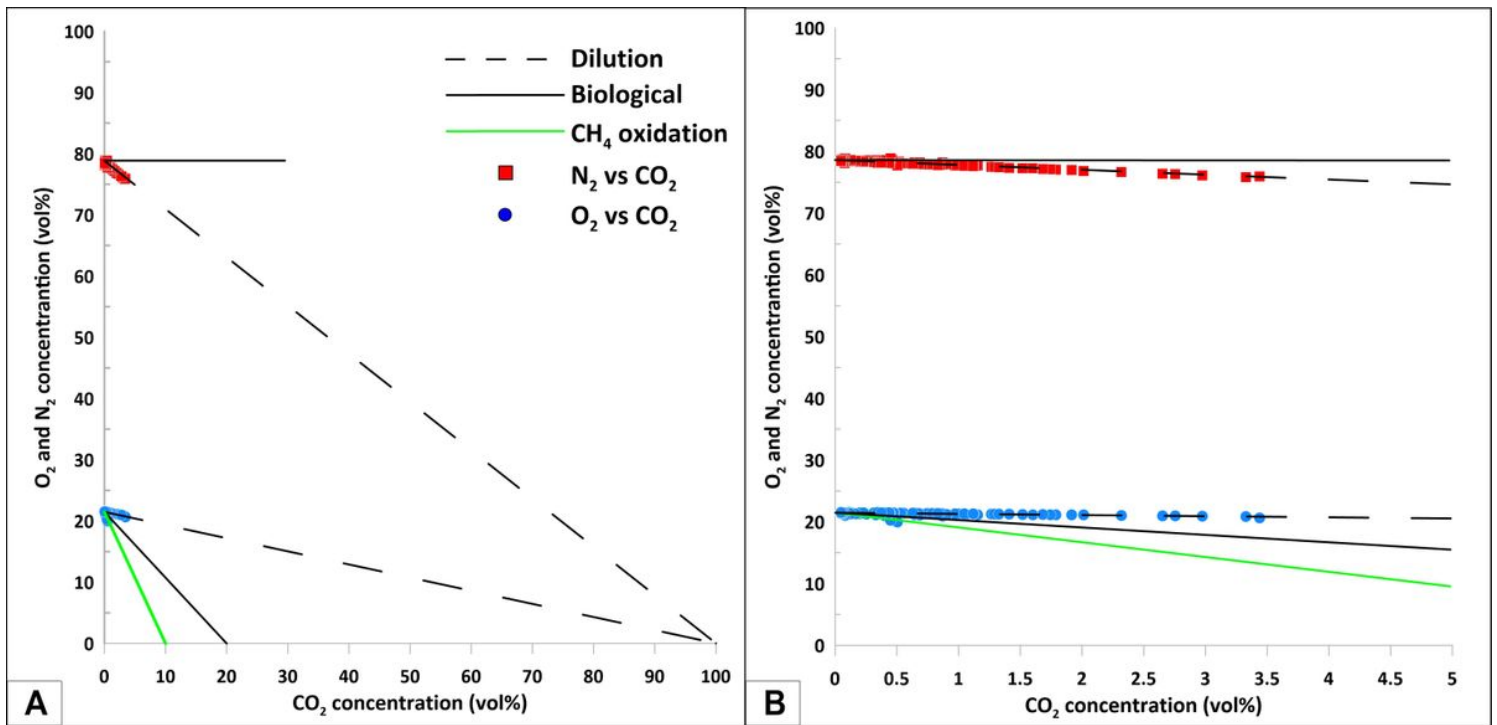


Figure 5

Scatter plot of O₂ and N₂ vs CO₂ (concentrations, vol%). The correlations between nitrogen and carbon dioxide, as well as oxygen and carbon dioxide, provide information about the tendency of data. Black solid lines highlight a biological source for the CO₂. Green lines show CO₂ derived by CH₄ oxidation, while dash lines indicate a dilution, an external contribution of CO₂ into the soil closed system (a). The same plot showing CO₂ concentrations up to 5% (b).

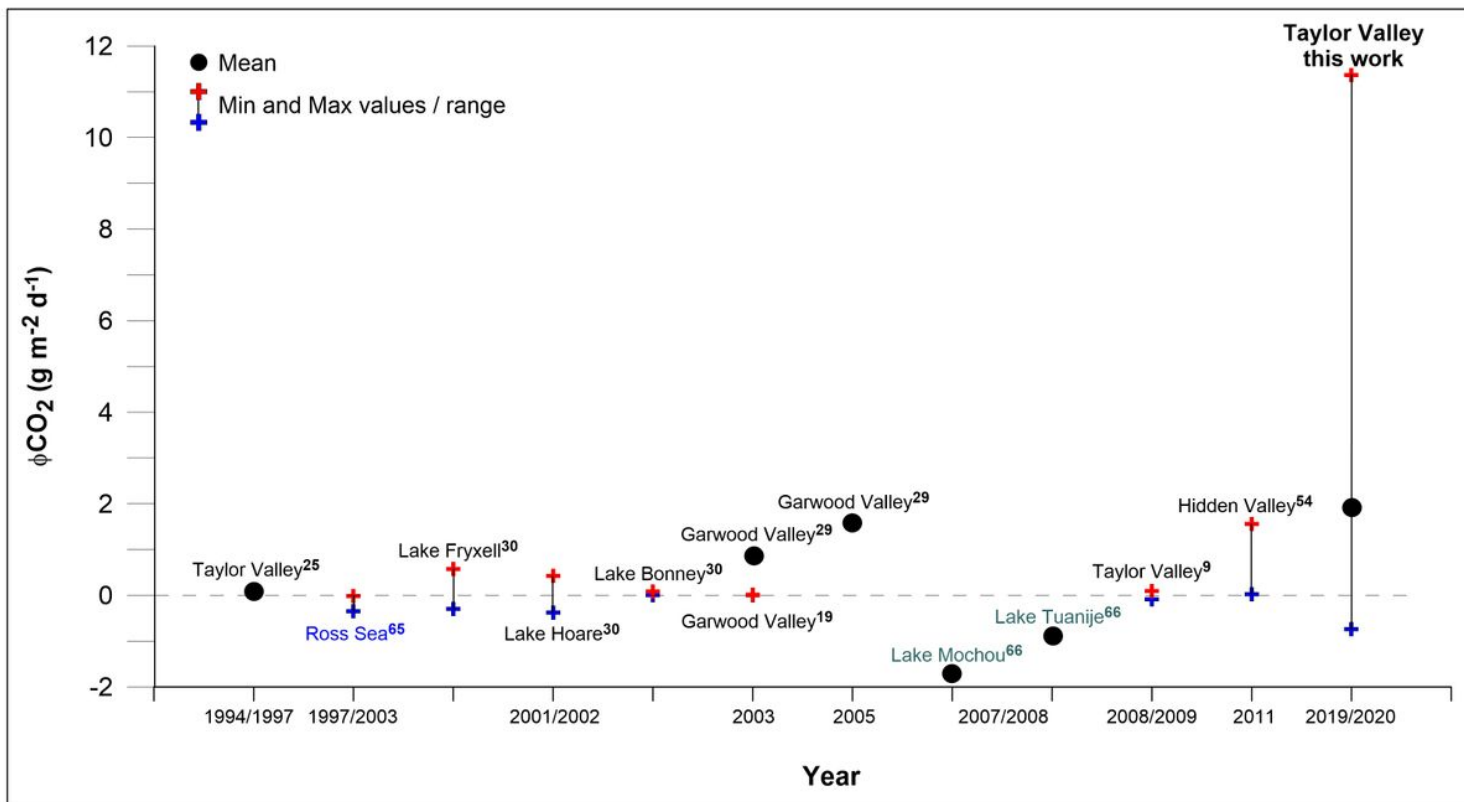


Figure 6

Summary diagram of ϕCO_2 measurements carried out since 1994 in Antarctica. The diagram shows CO_2 measurements performed in Antarctica by using various methods and in different environments. Measurements on dry soil (in black), lakes (in light blue) and the Ross Sea (in blue) are reported.

Supplementary Files

This is a list of supplementary files associated with this preprint. Click to download.

- [FIGURES1.jpg](#)
- [TABLES1.docx](#)
- [TABLES2.docx](#)